

Short communication

# Silica-based helical rod supporting guanosine compounds catalyzed asymmetric hetero-Diels–Alder reaction



Le Li <sup>a</sup>, Guangbin Zhang <sup>b</sup>, Benhua Huang <sup>a</sup>, Lin Ren <sup>a</sup>, Aquan Zheng <sup>a</sup>, Junjie Zhang <sup>a</sup>, Yang Sun <sup>a,\*</sup>

<sup>a</sup> Department of Applied Chemistry, School of Science, Xi'an Jiaotong University, Xi'an, No. 28, Xianning West Road, 710049, PR China

<sup>b</sup> School of Pharmacy, Health Science Center, Xi'an Jiaotong University, Xi'an, No. 76, Yanta West Road, 710061, PR China

## ARTICLE INFO

## Article history:

Received 20 December 2014

Received in revised form 17 January 2015

Accepted 20 January 2015

Available online 23 January 2015

## Keywords:

Helical rod

Internal channel

Guanosine

Immobilization

Hetero-Diels–Alder

## ABSTRACT

A series of silica-based helical rods were prepared and functionalized for immobilization of guanosine compounds in catalytic asymmetric hetero-Diels–Alder reaction. Nitrogen physisorption, electron microscopy and amino acid adsorption revealed that helical rod has a hierarchical structure including morphology and internal channels, and doping of sodium lactate facilitates porosity and internal chirality of synthetic rods. Catalysis revealed that guanosine derivatives were catalytically active, combination of guanosine with *L*-sodium lactate-doped rod was more enantioselective than that with zero- or *D*-sodium lactate-doped samples, and recycling of supported Schiff-base-guanosine was stable during six cycles.

© 2015 Elsevier B.V. All rights reserved.

## 1. Introduction

Asymmetric hetero-Diels–Alder (hDA) reaction gives chiral six-membered heterocycles, which showed values in synthetic and pharmaceutical chemistry [1]. Taking into account optical purity of product, separation of catalyst, as well as environmental concerns, design of catalyst for hDA had become an important task for both academic and industrial demands [2]. Previously, metal catalysts provided high conversion and enantioselectivity, like metallosalen [3], Schiff-base [4] or BINOL complexes [5]. But leaching of metal ions into product would become an unfavorable factor to commercialization [6]. Organocatalysis attracted attentions due to relief of metal toxicity, tolerance of water and air, and operational simplicity [7]. The  $\alpha,\alpha,\alpha',\alpha'$ -tetraaryl-1,3-dioxolane-4,5-dimethanol (TADDOL) [8], bis-sulfonamide derivatives [9] and oxazoline [10] brought about promising results, but heterogeneous catalysis was inadequate and deserved efforts [11].

Guanosine was composed of guanine and ribofuranose, which had unique biological [12] and material characters [13], but catalytic application was scarce. Actually, chiral centers of ribofuranose were hydroxylated and centralized, which were prone to inter- or intramolecular hydrogen bonds, eventually facilitating enantioselectivity. On the other hand, some nanosized helical silica had been applied as support in asymmetric catalysis [14], which confirmed chiral induction of helical configuration. Based on these progresses, this work aimed to develop helical silica for immobilization of guanosine as organocatalyst in

asymmetric hetero-Diels–Alder reaction, and to test synergetic effects between molecular catalyst and support.

## 2. Experimental

## 2.1. General

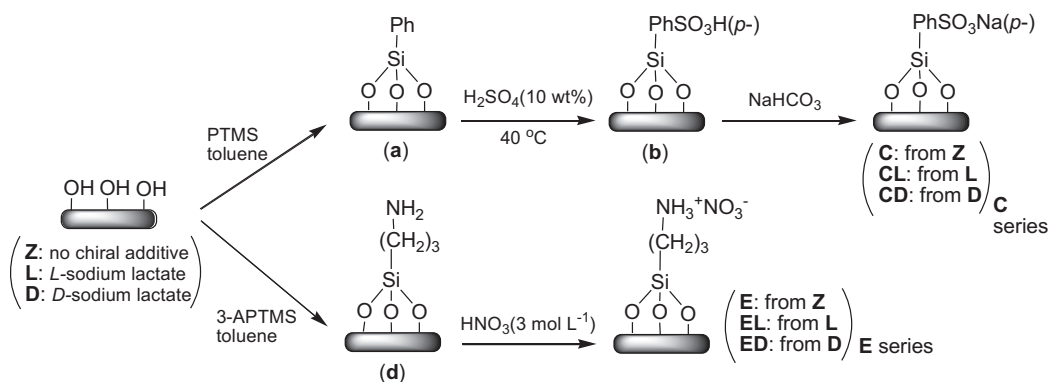
Starting materials and reagents were obtained as shown in Supplementary data, and disodium 3-*tert*-butyl-salicylaldehyde 5-sulfonate was synthesized according to literature [15]. <sup>1</sup>H NMR, ESI-HRMS, FT-IR and particle size were recorded on Bruker ADVANCE III (400 MHz), microOTOF-Q II, Bruker Tensor 27, and Zetasizer Nano ZS90 respectively. BET surface area, pore volume, pore radius and pore size distribution were recorded on Micromeritics ASAP 2020. Low-angle X-ray diffraction ( $2\theta$  at 0.5° to 10°) of powdered samples were reported on Philips X'Pert Pro diffractometer using Cu-K $\alpha$  radiation ( $\lambda$ , 1.5418 Å), with 0.05° s<sup>-1</sup> interval. X-ray photoelectron spectroscopy (XPS) was carried out on Kratos Axis Ultra DLD, using monochromatic Al K $\alpha$  X-ray (1486.6 eV) as irradiation source. Scanning electron microscopy (SEM) was performed on JEOL JSM-6700F at 20.0 kV with Au coating. Transmission electron microscopy (TEM) was tested on JEOL JEM-200CX at 120 kV.

Configuration of channels of Z, L and D was determined by enantioselective adsorption of chiral valine in aqueous solution (Scheme 1) [16]. In practice, sample (20 mg) and *L*- (or *D*-) valine (50 mg) were added to distilled water (20 mL), then vigorously stirred at 25 °C for 120 min. Concentration of *L*- (or *D*-) valine was measured by UV (210 nm, UV 1800, Shimadzu) under sampling at regular intervals.

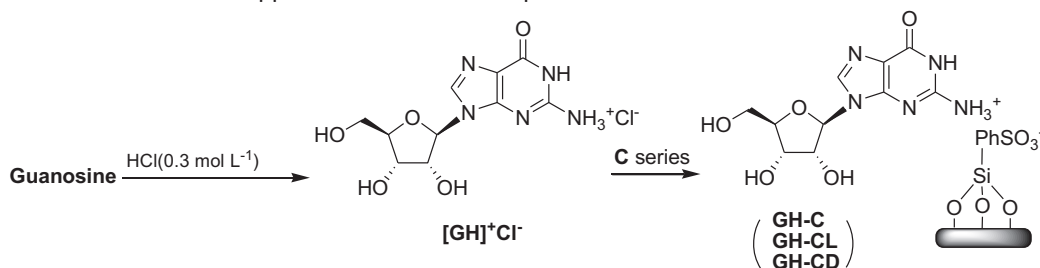
\* Corresponding author.

E-mail address: [sunyang79@mail.xjtu.edu.cn](mailto:sunyang79@mail.xjtu.edu.cn) (Y. Sun).

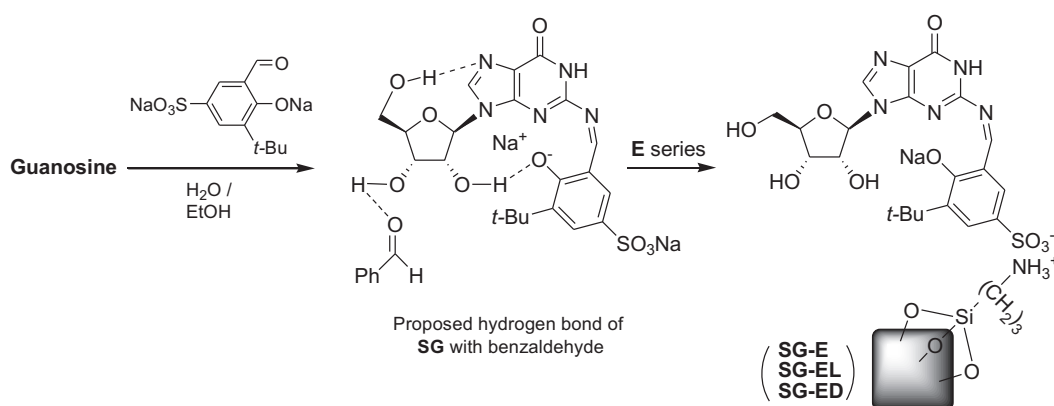
## Part 1. Functionalization of helical silica



## Part 2. Helical silica-supported Guanosine compounds



## Part 3. Helical silica-supported Schiff-base-Guanosine



Scheme 1. Synthesis of catalysts.

Adsorption percentage was calculated on Lambert–Beer's Law, then plotted as a function of time.

Thin layer chromatography (TLC) was tested on glass plates coated with GF<sub>254</sub> silica gel, coloration in phosphomolybdic acid (PMA)/ethanol solution (5 wt.%). Conversion and e.e. were determined by HPLC. System controller: Waters 1525, binary hplc pump; UV–vis detector: Waters 2998, photodiode array detector; UV: 254 nm for 2,3-dihydro-2-phenyl-4*H*-pyran-4-one (benzaldehyde), 2-(*p*-chlorophenyl)-2,3-dihydro-4*H*-pyran-4-one (4-chlorobenzaldehyde), 2-hexyl-2,3-dihydro-4*H*-pyran-4-one (heptaldehyde), 2-ethoxyformyl-2,3-dihydro-4*H*-pyran-4-one (ethyl glyoxylate), obtained after scanning 200–400 nm. Daicel Chiralcel OD-H, size: 150 mm × 4.6 mm; particle: 5 μm; mobile phase: *n*-hexane/2-propanol, 90/10, v/v; rate: 0.5 mL min<sup>-1</sup>; column temperature: 300 K; pressure: 3.0–3.5 MPa; sample concentration: 0.5 mg mL<sup>-1</sup> in *n*-hexane; injection: 10 μL.

## 2.2. Synthesis

### 2.2.1. Synthesis of supports

Sample Z was synthesized when hexadecyltrimethylammonium bromide and ammonia solution (25 wt.%) were used as surfactant and

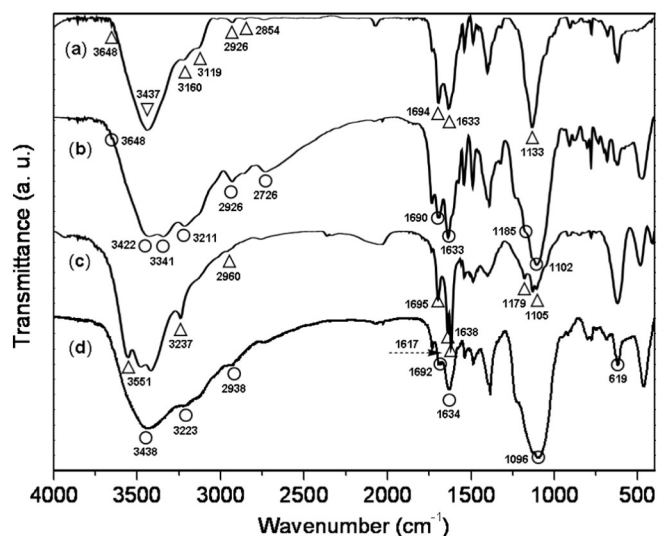


Fig. 1. FT-IR of guanosine (a), GH-CL (b), SG (c) and SG-EL (d).

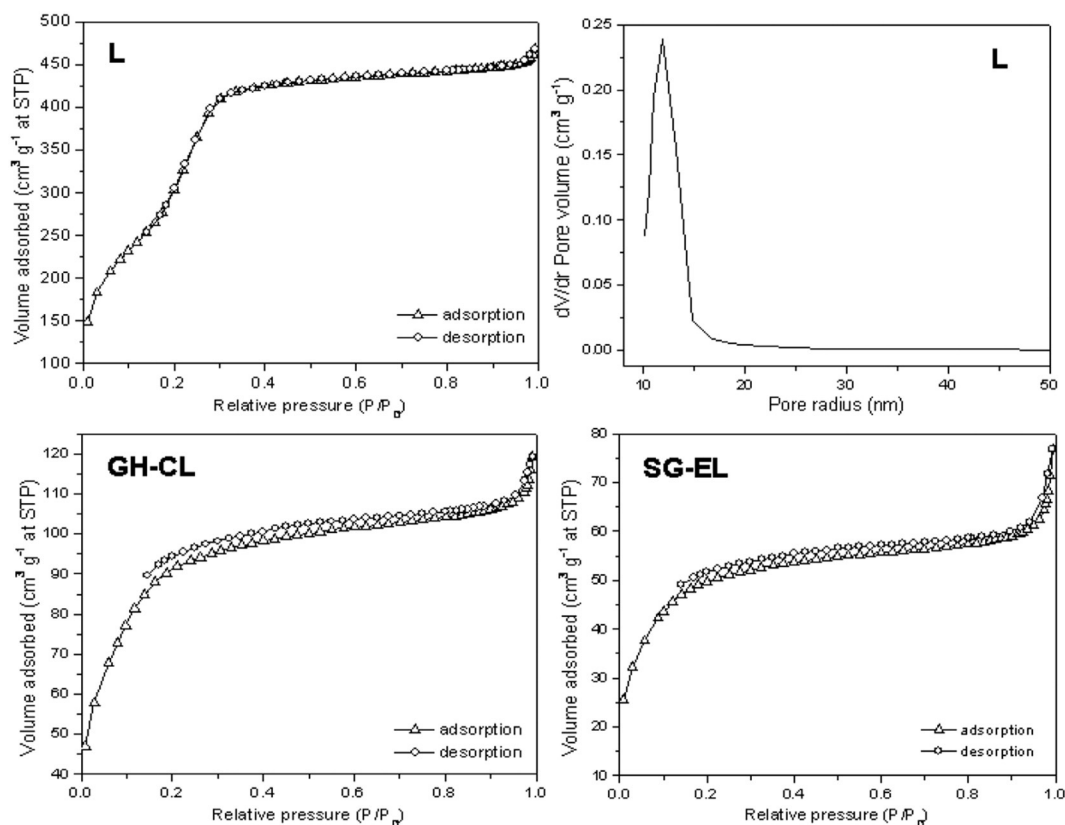


Fig. 2. N<sub>2</sub> adsorption–desorption isotherms of L, GH-CL and SG-EL and pore size distribution of L.

co-surfactant, and templates were removed by calcination [17]. Our attempt was loading of chiral sodium lactate in order to facilitate internal chirality. Synthesis of L and D, phenylsulfonation (C, CL, CD) [18] and ammoniation (E, EL, ED) were shown in Supplementary data.

### 2.2.2. Synthesis of helical silica-supported guanosine compounds

[GH]<sup>+</sup>Cl<sup>−</sup> was prepared in HCl solution, and GH-C (GH-CL or GH-CD) was obtained by ion-exchanging. SG was synthesized in H<sub>2</sub>O/ethanol solution, and SG-E (SG-EL or SG-ED) was obtained by ion-exchanging too. Details were shown in Supplementary data.

### 2.3. Catalysis

Aldehyde (1.0 mmol), Danishefsky's diene (1.0 mmol), molecular sieve (50 mg, 4 Å) and catalyst (20 mol% N or Na based on diene) were added to dichloromethane (3.0 mL), then stirred at 0 °C and monitored by TLC/PMA (petroleum ether, R<sub>f</sub> of Danishefsky's diene: 0.3; R<sub>f</sub> of benzaldehyde, heptaldehyde, ethyl glyoxylate: 0.48, 0.64, invisible; R<sub>f</sub> of above hDA products: 0.56, 0.72, 0.70 accordingly; petroleum ether/ethyl acetate, v/v, 3/1, R<sub>f</sub> of Danishefsky's diene,

4-chlorobenzaldehyde, its hDA product: 0.50, 0.67, 0.75). After 6 h, three drops of trifluoroacetic acid were added and further stirred for 1 h. Mixture was concentrated, and extracted by *n*-hexane (3 × 5 mL), and the left catalysts were reloaded with consumables for recycling. Hexane layer was concentrated and purified by SiO<sub>2</sub> (200–300 mesh, petroleum ether), then tested on HPLC.

## 3. Results and discussion

### 3.1. Characterization

Guanosine showed 3648 (O–H of sec-alcohol), 3160 and 3119 (furyl), 2926 and 2854 (C–H on methylene), 1694 (–CONH–), 1633 (C=N on guanine), and 1133 (C–O–C) cm<sup>−1</sup> (a, Fig. 1), which were still visible in GH-CL without significant shifts (b). The 3437 cm<sup>−1</sup> of

**Table 1**  
Textural parameters of synthetic samples.

Sample	S <sub>BET</sub> <sup>a</sup>	PV <sup>b</sup>	PR <sup>c</sup>	ρ <sup>d</sup>	d <sub>s</sub> <sup>e</sup>	d <sub>w</sub> <sup>f</sup>
Z	958.2	6.4 × 10 <sup>−1</sup>	12.9	0.2	31.3	175.7
L	1372.9	8.6 × 10 <sup>−1</sup>	12.9	1.0	4.3	89.6
GH-CL	297.5	9.7 × 10 <sup>−2</sup>	16.9	0.7	20.1	299.9
SG-EL	161.8	6.8 × 10 <sup>−2</sup>	24.3	1.0	37.0	44.7
SG-E	13.2	4.2 × 10 <sup>−2</sup>	80.3	0.8	454.5	102.6

<sup>a</sup> Surface area (m<sup>2</sup> g<sup>−1</sup>) determined by BET method based on N<sub>2</sub> adsorption.

<sup>b</sup> Pore volume (cm<sup>3</sup> g<sup>−1</sup>), BJH method on N<sub>2</sub> adsorption.

<sup>c</sup> Pore radius (nm), BJH method on N<sub>2</sub> adsorption.

<sup>d</sup> Bulk density (g cm<sup>−3</sup>).

<sup>e</sup> Crystallite size (nm) based on BET surface area: d<sub>s</sub> = 6 / (S<sub>BET</sub> · ρ), ρ bulk density.

<sup>f</sup> Diameter of particle in CH<sub>2</sub>Cl<sub>2</sub> (nm).

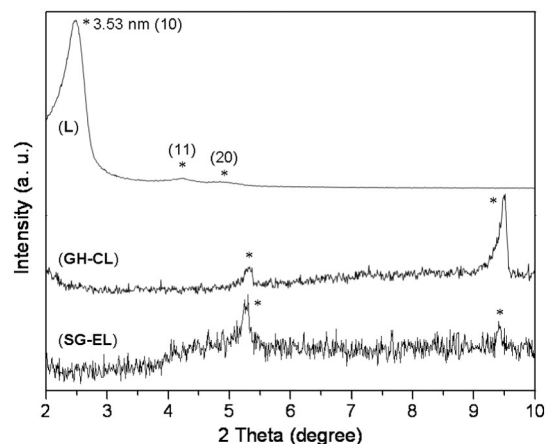


Fig. 3. Low-angle XRD of L, GH-CL and SG-EL.

**Table 2**

Binding energy and surface atomic composition of O, C, Si and N species in synthetic samples.

Sample	O (1s)	C (1s)	Si (2p)	N (1s) or Na (1s)
Z	530.0 (26.7) <sup>a</sup>	282.0 (55.2)	101.0 (17.7)	–
L	530.0 (42.3)	282.0 (23.4)	101.0 (34.1)	–
CL	529.0 (53.0)	281.0 (20.1)	100.0 (35.7)	1069.0 (0.9) <sup>b</sup>
GH-CL	529.0 (32.9)	281.0 (39.0)	100.0 (25.2)	396.0 (2.7)
GH-CD	529.0 (33.5)	281.0 (38.3)	100.0 (23.6)	396.0 (2.1)
GH-C	529.0 (27.9)	281.0 (59.1)	100.0 (18.5)	396.0 (1.1)
EL	529.0 (36.1)	281.0 (18.5)	100.0 (25.7)	396.0 (17.9)
SG-EL	529.0 (17.6)	282.0 (68.3)	99.0 (4.9)	396.0 (9.0)
SG-ED	529.0 (20.1)	282.0 (66.9)	99.0 (5.1)	396.0 (6.7)
SG-E	529.0 (28.5)	281.0 (48.1)	100.0 (18.0)	396.0 (5.3)

<sup>a</sup> Binding energy (eV), along with atomic percentage (at.%) in parentheses.

<sup>b</sup> Binding energy (eV) and atomic percentage (at.%) of Na based on its 1s photoelectron, other data in this column represented those of N (1s).

guanosine ( $-\text{NH}_2$ , a) was broadened at  $3422\text{ cm}^{-1}$  (b), and the new broad band appeared at  $3000\text{--}2000\text{ cm}^{-1}$  (b), which both witnessed formation of  $-\text{NH}_3^+$ . The  $1185$  and  $1102\text{ cm}^{-1}$  indicated anti-symmetric and symmetric stretching of  $-\text{SO}_3^-$  (b) [15]. Therefore, acidified guanosine was linked with CL.

Vibrations at  $3551$  (O–H of alcohols, with hydrogen bond association),  $3237$  (furyl),  $2960$  (C–H on methyl),  $1695$  ( $-\text{CONH}-$ ),  $1638$  (C=N on guanine),  $1617$  (C=N),  $1179$  and  $1105$  ( $-\text{SO}_3^-$ )  $\text{cm}^{-1}$  proved formation of Schiff-base-guanosine (c). After immobilization, the  $3223$

(furyl),  $2938$  (C–H on methyl),  $1692$  ( $-\text{CONH}-$ ) and  $1634$  (C=N, guanine)  $\text{cm}^{-1}$  were still visible (d). In comparison with EL (Fig. S1, Supplementary data), the broad adsorption between  $3000$  and  $2500\text{ cm}^{-1}$  ( $-\text{NH}_3^+$ ),  $1096$  (Si–O) and  $619$  (Si–C)  $\text{cm}^{-1}$  witnessed linkage of SG with EL (d).

Both Z and L showed type II isotherm and large surface area (Fig. S2, Fig. 2 and Table 1), indicating that they had uniform channel-like mesopores [17,19]. Sodium lactate remarkably gave a new level of surface area ( $1372.9$  vs.  $958.2\text{ m}^2\text{ g}^{-1}$ , Table 1), being ascribed to its unique template effect. Accordingly, modification on L looked better than that on Z in terms of surface area and pore volume (Table 1). GH-CL had type II isotherm (Fig. 2) without ordered pore distribution (Fig. S2) [19], along with lower surface area and pore volume than L (Table 1), because guest molecules occupied, blocked, or sealed internal channels of L. SG-EL showed the same tendency on porosity (Table 1).

L showed hexagonal symmetry similar to Z, where  $10$ ,  $11$ , and  $20$  diffractions were recognizable (Figs. 3 and S3, scattering of  $0.5^\circ\text{--}2.0^\circ$  omitted for clarity) [17]. Lattice constant (a) of L ( $3.53\text{ nm}$ , Fig. 3) was smaller than that of Z ( $3.74\text{ nm}$ , Fig. S3). Therefore, sodium lactate did not destroy hexagonal symmetry but promote porosity. Compared with L, GH-CL and SG-EL showed new basal spacing at  $1.66\text{ nm}$  ( $2\theta$ ,  $5.32^\circ$ ) and  $1.67\text{ nm}$  ( $2\theta$ ,  $5.30^\circ$ ) respectively, revealing that silica reagent and guanosine reside at lattice plane of L (Fig. 3).

Neither Z nor L showed detectable photoelectrons of nitrogen which revealed that nitrogen-containing template was completely removed after calcination (Table 2). Sodium lactate accelerated removal of

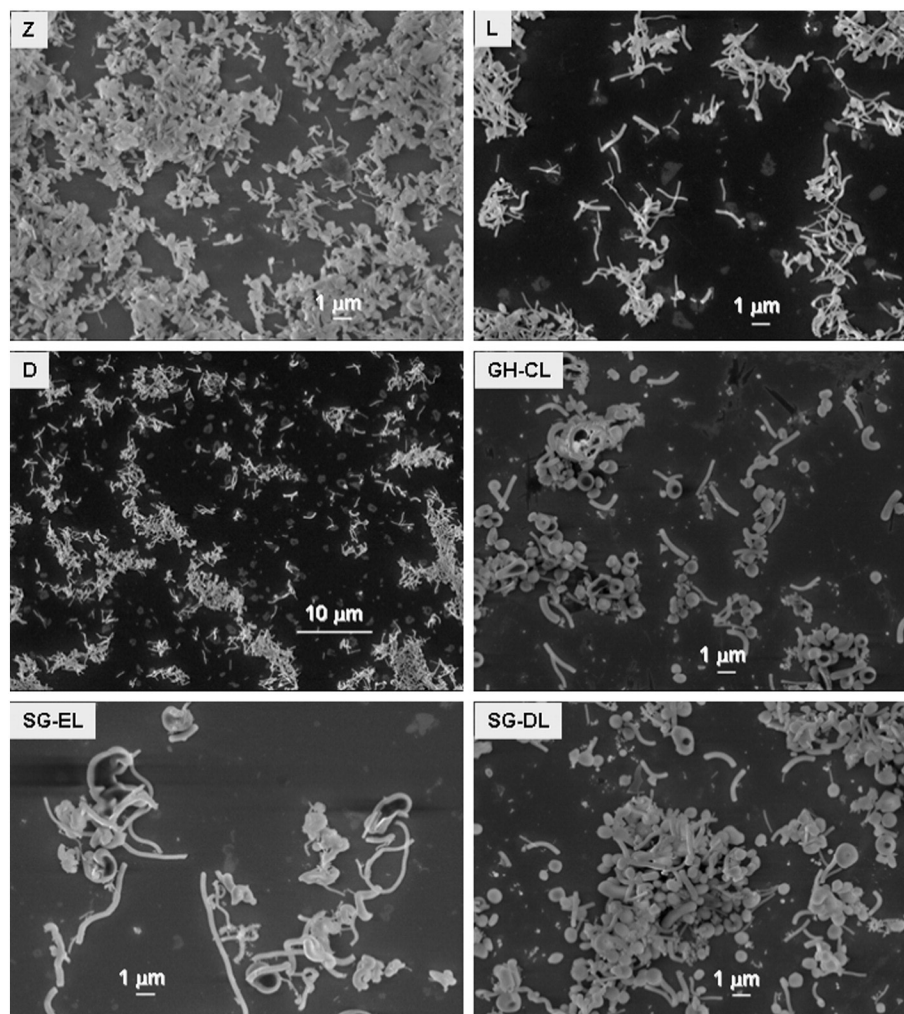


**Fig. 4.** SEM of Z, L, D, GH-CL, SG-EL and SG-DL.

templates, so carbon content was halved, while oxygen and silicon increased sharply (L vs. Z, Table 2). Binding energy and atomic percentage from L to CL then GH-CL demonstrated that silica reagent and guanosine were attached to the surface of L, a similar tendency was found on L to EL then SG-EL (Table 2). Based on nitrogen content, loading of guanosine had an order: GH-CL > GH-CD > GH-C (Table 2), reflecting influence of sodium lactate too.

Sample Z was composed of twisted rods having a length of 0.2–1  $\mu\text{m}$  (Z, Fig. 4). Addition of chiral sodium lactate produced longer helical rods, where L showed length of 0.2–3  $\mu\text{m}$ , pitch of 0.5–1.5  $\mu\text{m}$ , as well as offset (distance from spiral axis to center of rod) of 50–250 nm (L vs. Z). L and D had both right- and left-handed morphology, demonstrating that sodium lactate may not work with morphology (Fig. 4). GH-CL, SG-EL and SG-DL degraded by different degrees perhaps due to hydrolysis in synthesis (Fig. 4, Section 2.2.2) [20]. SG-EL looked more helical than GH-CL and SG-DL, but became bolder and longer than L (Fig. 4). TEM confirmed that Z, L, GH-CL and SG-EL were solid rods instead of hollow tubes (Fig. S4). Based on enantioselective adsorption of valine (Fig. S5), Z preferred *L*-valine more than *D*-valine, indicating excessive left-handed channels [16]. But both *L*- and *D*-sodium lactate changed adsorption priority of Z, which meant that L and D were internally right-handed [16].

### 3.2. Catalysis

Catalyst blank showed 3% conversion, indicating that molecular sieve (4 Å) was catalytically active to some extent (entry 1, Table 3), which also proved that sulfonated silica (CL) was inactive (entry 2). EL improved conversion perhaps owing to ammoniums, while e.e. of 9% meant that channels of EL were enantioselective (entry 3).

Acidified guanosine showed improved conversion and enantioselectivity than guanosine (entries 5 vs. 4), perhaps owing to ammonium,

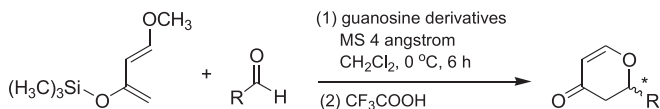
whose role was similar to the secondary amine-catalyzed hetero-Diels-Alder [7]. After immobilization, acidified guanosine promoted e.e. (entries 7, 8, 12 vs. 5), probably because guanosine was confined in a more rigid environment. Recycling demonstrated that GH-CL degrades slowly, but major configuration of product was maintained (entry 8).

L and D were both internally right-handed while Z left-handed, but a combination of  $[\text{GH}]^+\text{Cl}^-$  with CL was more enantioselective than that with CD or Z (entries 8 vs. 12 and 7). In addition, the same level of e.e. and lower conversion were obtained in heptaldehyde and ethyl glyoxylate (entries 10 and 11), and much reduced results were obtained in 4-chlorobenzaldehyde (entry 9), but acetophenone was completely inert, illustrating that aldehyde was more active than ketone [1,7].

Condensation of guanosine with salicylaldehyde gave 65% conversion as well as 39% e.e., higher than guanosine and  $[\text{GH}]^+\text{Cl}^-$  (entries 13 vs. 4 and 5). In view of TADDOL [24], salicylaldehyde might provide an intramolecular hydrogen bond between phenolic oxygen with hydroxyl of guanosine, then intermolecular hydrogen bond between benzaldehyde and guanosine looked more exclusive leading to improved stereoselectivity (Scheme 1).

Immobilization of SG improved enantioselectivity, because configuration of SG was confined in channels of E, EL or ED (entries 15, 16, 20 vs. 13). SG-E showed a conversion less than half of SG-EL and SG-ED (entries 15 vs. 16 and 20), due to its poor surface area (Table 1). SG-EL provided better e.e. than SG-ED (entries 16 vs. 20), probably because L showed a much larger adsorption difference between *L*- and *D*-sodium lactates than D (Fig. S5). Recycling of SG-EL was satisfactory during six cycles that witnessed that degradation was not very sharp in dichloromethane (entry 16). Heptaldehyde and ethyl glyoxylate were still moderate substrates (entries 18 and 19). 4-Chlorobenzaldehyde was not as good as benzaldehyde either (entries 17 vs. 16), perhaps because electron-withdrawing of chlorine

**Table 3**  
Asymmetric hDA reaction of Danishefsky's diene with aldehydes catalyzed by guanosine derivatives.



Entry <sup>a</sup>	Catalyst	Aldehyde (R) <sup>b</sup>	Conversion <sup>c</sup> (%)	E.e. <sup>d</sup> (%)	TOF <sup>e</sup> (h <sup>-1</sup> )
1	None	Ph	3	0	–
2	CL	Ph	2	0	$1.6 \times 10^{-2}$
3	EL	Ph	6	9 (R)	$5.0 \times 10^{-2}$
4	Guanosine	Ph	10	7 (R)	$8.3 \times 10^{-2}$
5	$[\text{GH}]^+\text{Cl}^-$	Ph	39	11 (R)	$3.2 \times 10^{-1}$
6	$[\text{GH}]^+\text{Cl}^-$	<i>p</i> -ClPh	6	12	$5.0 \times 10^{-2}$
7	GH-C	Ph	37	19 (R)	$3.0 \times 10^{-1}$
8	GH-CL	Ph	55 (51,55,49,45,30)	33 (39,35,20,22,27) (R)	$4.5 \times 10^{-1}$
9	GH-CL	<i>p</i> -ClPh	10	15	$8.3 \times 10^{-2}$
10	GH-CL	<i>n</i> -C <sub>6</sub> H <sub>13</sub>	30	45	$2.5 \times 10^{-1}$
11	GH-CL	CH <sub>3</sub> CH <sub>2</sub> OC=O	31	32	$2.5 \times 10^{-1}$
12	GH-CD	Ph	57	16 (R)	$4.7 \times 10^{-1}$
13	SG	Ph	65	39 (R)	$5.4 \times 10^{-1}$
14	SG	<i>p</i> -ClPh	27	30	$2.2 \times 10^{-1}$
15	SG-E	Ph	20	59 (R)	$1.6 \times 10^{-1}$
16	SG-EL	Ph	71 (70,73,66,50,40)	61 (60,50,57,63,47) (R)	$5.9 \times 10^{-1}$
17	SG-EL	<i>p</i> -ClPh	31	40	$2.5 \times 10^{-1}$
18	SG-EL	<i>n</i> -C <sub>6</sub> H <sub>13</sub>	45	29	$3.7 \times 10^{-1}$
19	SG-EL	CH <sub>3</sub> CH <sub>2</sub> OC=O	26	37	$2.1 \times 10^{-1}$
20	SG-ED	Ph	51	55 (R)	$4.2 \times 10^{-1}$

<sup>a</sup> Conditions: Danishefsky's diene (1.0 mmol), aldehyde (1.0 mmol), catalyst (20 mol% of N based on diene), MS 4 Å (50 mg), and CH<sub>2</sub>Cl<sub>2</sub> (3 mL). For entry 2, catalyst (20 mol% of Na based on diene).

<sup>b</sup> Benzaldehyde, 4-chlorobenzaldehyde, heptaldehyde, and ethyl glyoxylate as four substrates.

<sup>c</sup> Molar ratio of product to original diene, values in parenthesis represented recycling data.

<sup>d</sup> Enantiomeric excess. Retention time (min): product of benzaldehyde, 3.570 (R) and 3.880 (S), configuration determined by comparison of retention time from literature [21]; product of 4-chlorobenzaldehyde, 3.598 (major) and 3.918 (minor) [21]; product of heptaldehyde, 3.942 (major) and 7.289 (minor) [21,22]; product of ethyl glyoxylate, 3.944 (major) and 7.399 (minor) [23], no absolute configuration determined for three substrates.

<sup>e</sup> Turnover frequency of cycle fresh,  $\text{mol}_{\text{product}}/\text{mol}_{(\text{N or Na})} (6 \text{ h})^{-1}$ .

weakened hydrogen bond between aldehyde and guanosine. Based on the data obtained so far, benzaldehyde was the most appropriate in this system.

#### 4. Conclusions

Addition of chiral sodium lactate facilitated porosity and internal chirality of silica materials through sol–gel synthesis. Guanosine derivatives were catalytically active in asymmetric hetero-Diels–Alder reaction, while their immobilization into helical silica further improved enantioselectivity and conversion. This study emphasized synergistic effects of biological molecule with chiral support in asymmetric catalysis.

#### Acknowledgments

This study was supported by Shaanxi Higher Education Teaching Reform Project (No. 13BY02, Cultivation of Creative Ability of Scientific Research for the Undergraduate), and the Fundamental Research Funds for the Central Universities (No. xjj2014005).

#### Appendix A. Supplementary data

Starting materials and reagents, as well as the synthesis, characterization, FT-IR, nitrogen physisorption and pore size distribution, low-angle XRD, TEM, amino acid adsorption of intermediates, along with  $^1\text{H}$  NMR of hDA products, ESI analysis of catalytic product, and template of chiral HPLC were included. Supplementary data associated with this article can be found, in the online version, at <http://dx.doi.org/10.1016/j.catcom.2015.01.016>.

#### References

- [1] H. Pellissier, *Tetrahedron* 65 (2009) 2839–2877.
- [2] D. Lanari, F. Montanari, F. Marmottini, O. Piermatti, M. Orrù, L. Vaccaro, *J. Catal.* 277 (2011) 80–87.
- [3] S.E. Schaus, J. Brånalt, E.N. Jacobsen, *J. Org. Chem.* 63 (1998) 403–405.
- [4] Q. Fan, L. Lin, J. Liu, Y. Huang, X. Feng, G. Zhang, *Org. Lett.* 6 (2004) 2185–2188.
- [5] J. Long, J. Hu, X. Shen, B. Ji, K. Ding, *J. Am. Chem. Soc.* 124 (2002) 10–11.
- [6] F. Bellezza, A. Cipiciani, U. Costantino, F. Fringuelli, M. Orrù, O. Piermatti, F. Pizzo, *Catal. Today* 152 (2010) 61–65.
- [7] M.J. Gaunt, C.C.C. Johansson, A. McNally, N.T. Vo, *Drug Discov. Today* 12 (2007) 8–27.
- [8] Y. Huang, A.K. Unni, A.N. Thadani, V.H. Rawal, *Nature* 424 (2003) 146.
- [9] W. Zhuang, T.B. Poulsen, K.A. Jørgensen, *Org. Biomol. Chem.* 3 (2005) 3284–3289.
- [10] S. Rajaram, M.S. Sigman, *Org. Lett.* 7 (2005) 5473–5475.
- [11] A. Puglisi, M. Benaglia, R. Annunziata, V. Chiroli, R. Porta, A. Gervasini, *J. Org. Chem.* 78 (2013) 11326–11334.
- [12] M. Nath, H. Singh, G. Eng, X. Song, *Inorg. Chem. Commun.* 14 (2011) 1381–1385.
- [13] M. Devetak, S. Masiero, S. Pieraccini, G.P. Spada, M. Čopič, I.D. Olenik, *Appl. Surf. Sci.* 256 (2010) 2038–2043.
- [14] C.I. Fernandes, M.S. Saraiva, T.G. Nunes, P.D. Vaz, C.D. Nunes, *J. Catal.* 309 (2014) 21–32.
- [15] Z. Zhang, F. Guan, X. Huang, Y. Wang, Y. Sun, *J. Mol. Catal. A Chem.* 363–364 (2012) 343–353.
- [16] Z. Guo, Y. Du, Y. Chen, S.-C. Ng, Y. Yang, *J. Phys. Chem. C* 114 (2010) 14353–14361.
- [17] Y. Han, L. Zhao, J.Y. Ying, *Adv. Mater.* 19 (2007) 2454–2459.
- [18] H. Zhang, Y. Zhang, C. Li, *J. Catal.* 238 (2006) 369–381.
- [19] K.S.W. Sing, D.H. Everett, R.A.W. Haul, L. Moscou, R.A. Pierotti, J. Rouquérol, T. Siemieniowska, *Pure Appl. Chem.* 57 (1985) 603–619.
- [20] A. Galarneau, M. Nader, F. Guenneau, F.D. Renzo, A. Gedeon, *J. Phys. Chem. C* 111 (2007) 8268–8277.
- [21] K. Aikawa, R. Irie, T. Katsuki, *Tetrahedron* 57 (2001) 845–851.
- [22] M. Mellah, B. Ansel, F. Patureau, A. Voiturier, E. Schulz, *J. Mol. Catal. A Chem.* 272 (2007) 20–25.
- [23] C. Qian, L. Wang, *Tetrahedron Lett.* 41 (2000) 2203–2206.
- [24] R.A. Ocampo, J. Scoccia, A.R. Costantino, M.G.M. Schneider, D.C. Gerbino, A.E. Zúñiga, M. Pereyra, L.C. Koll, S.D. Mandolesi, *Catal. Commun.* 58 (2015) 209–214.